Relational Tension, Topology, and Quasi-Particles in RZS: A Conservative Route with Negative and Positive Gates

Felipe Gianini Romero
Independent Researcher, Brazil
lipegianini88@gmail.com

May 2026

Abstract

This manuscript organizes a sequence of exploratory tests to investigate whether the Relational Zero State (RZS) framework can support a formal route from relational tension to particle-like objects. The conclusion is deliberately restricted. Pure relational tension generates criticality, localized modes, and partial tensional mass, but tends to produce pinned defects rather than mobile particles. The route that survives the strongest gates requires a compact phase, topological charge, and, in two dimensions, a relational gauge connection. In the 1D sector, topological kinks display finite mass, mobility, interaction, internal modes, and transport under sufficient Romero stability. In the 2D sector, global vortices fail because their energy diverges logarithmically; gauged vortices have finite energy and static stability, but full 2D mobility still depends on gauge-consistent integrators and remains open. The manuscript does not claim a derivation of Standard Model particles. Its contribution is a route toward relational topological quasi-particles, with explicit limits of validity and falsifiability.

Summary for non-specialists. The starting question is simple: if relations between points carry tension, can that tension generate something resembling fields and particles? The tests suggest that tension helps, but it is not enough by itself. With tension alone, localized patterns appear, but they remain trapped in the medium, behaving like defects. The decisive step is to treat the phase of the field as compact and to allow it to carry a topological charge. Then solitons appear: objects that preserve shape, charge, and mass. In two dimensions, however, a vortex has finite mass only when a gauge connection cancels the long-range energy tail. The promising route is therefore not "tension becomes a particle," but rather: relational stability supports a coherent medium, and within that medium topological charges can behave as quasi-particles.

1 Scope and rule of honesty

I do not claim in this text that RZS derives the electron, muon, tau, quarks, spin, or the Standard Model. The claim defended here is narrower:

> A topological-relational sector of RZS can support solitonic quasi-particles: objects with topological charge, finite mass, conditional mobility, interaction, and internal modes, provided that the relational stability of the medium remains above an operational threshold.

The word "particle" is used only when the object passes minimal gates: finite mass, localization, conserved charge or number, mobility, dynamical stability, coherent interaction, and robustness under perturbations. When a gate fails, the text states that it fails.

2 Operational conventions and normalizations

The tests below use a few conventions that matter for reproducibility.

First, all transport tables distinguish displacement, relative width growth, and energy drift as separate observables. The width column is dimensionless, and the energy-drift column is a relative variation written in scientific notation.

Second, the compact-phase sector uses an explicit wrap operation before defining the XY energy. This prevents ambiguity in angular differences modulo 2π.

Third, different 2D energies are not compared unless they belong to the same normalization. The symbols E_{ansatz}, E_{radial}, and E_{lattice} refer to different functionals or discretizations.

Fourth, the relation $E(v) = \gamma M$ is used only as a consistency test for the sine-Gordon sector. It is expected from Lorentz invariance and is not, by itself, independent evidence for RZS.

Fifth, the normalized Romero stability uses a homogeneous reference graph with the same topology, the same number of nodes, the same boundary conditions, and homogeneous weights equal to the mean weight $B = \langle W \rangle$.

3 Romero Law and relational tension

The Romero Law of Relational Stability is used in the operational form

$$\sigma_{\text{rel}} = k\frac{B}{I\tau}, \tag{1}$$

where k fixes the dimensional scale or units of the observable being compared. In the dimensionless comparisons used throughout this manuscript, $k = 1$, so that

$$\sigma_{\text{rel}}^{(0)} = \frac{B}{I\tau}. \tag{2}$$

Here B measures effective update capacity, I measures informational noise or load, and τ measures latency. The simple reading is that stability increases with update capacity and decreases when the system becomes noisy or slow.

The minimal relational tension between two connected nodes i, j, with link weight W_{ij} and states ϕ_i, ϕ_j, is

$$T_{ij} = \frac{1}{2}W_{ij}(\phi_i - \phi_j)^2. \tag{3}$$

The total tension energy on a graph is the discrete Dirichlet energy

$$E_T[W, \phi] = \frac{1}{2}\sum_{ij} W_{ij}(\phi_i - \phi_j)^2. \tag{4}$$

Intuition. If two points are strongly connected but try to occupy very different states, the link between them becomes tense. This tension does not create energy from nothing; it measures the cost of maintaining a difference inside a connection.

When the network is adaptive, I use a weak weight update of the form

$$W_i(t + \Delta t) = \frac{\bar{W}}{\langle W_i(t)e^{-\eta T_i(t)\Delta t}\rangle} W_i(t)e^{-\eta T_i(t)\Delta t}. \tag{5}$$

Here η is the tension-adaptation rate. The multiplicative factor normalizes the mean weight to $\bar{W}$; angle brackets $\langle\cdot\rangle$ denote an average over links. This prevents the tests from confusing structural stability with a trivial global decrease in the scale of W.

4 First tested route: spectral modes induced by tension

The initial hypothesis was that graph-Laplacian modes could act as pre-particle candidates:

$$L\psi_n = \lambda_n \psi_n, \tag{6}$$

with proxy masses such as

$$m_n \propto \sqrt{\lambda_n}, \tag{7}$$

or localization measured by the inverse participation ratio,

$$\mathrm{IPR}_n = \sum_i |\psi_n(i)|^4. \tag{8}$$

The gates showed that tension generates criticality and localization, but also pinning. The pure spectral mass drifted with system size. The local tensional mass,

$$m_T^2 \equiv \epsilon_n T_{\mathrm{avg},n}, \tag{9}$$

was more stable, but still did not yield mobility. The conclusion of this first route was negative for mobile particles.

Status. Pure tension is useful for generating criticality and localized modes, but it is insufficient for mobile particles.

Table 1: Summary of the initial gates with pure tension.

Gate	Result	Interpretation
Modes of L	Localization appeared, mass did not converge	Critical soft modes, not massive particles
IPR and adjacent gap	Gap closed with N	Fails as an isolated particle
Tensional operator $L + \kappa\,\mathrm{diag}(t)$	Mass improved	Local tension is a real ingredient
Mobility under impulse	Modes remained pinned	Defects, not mobile particles

5 The route that survives: compact phase and topological charge

The next route introduced a compact phase ϕ and topological charge. In the 1D sector, the sine-Gordon-like energy weighted by relational rigidity is

$$E[\phi] = \frac{1}{2}\sum_i W_i(\phi_{i+1} - \phi_i)^2 + U_0 \sum_i (1 - \cos\phi_i). \tag{10}$$

The topological charge is

$$Q = \frac{\phi(+\infty) - \phi(-\infty)}{2\pi}. \tag{11}$$

A kink has $Q = 1$; an antikink has $Q = -1$.

In the homogeneous case, the kink mass obeys

$$M_Q \simeq 8\sqrt{KU_0}\,|Q|. \tag{12}$$

This law was verified numerically and used as an implementation check.

6 Kink transport in a relational medium

Table 2 separates displacement, relative width, and energy drift. The width column is dimensionless; the drift column is the relative variation of energy.

Intuition. The object moves cleanly when the medium is weakly disordered. When the medium becomes too irregular, the object can still exist, but it loses clean transport: it becomes trapped or deformed.

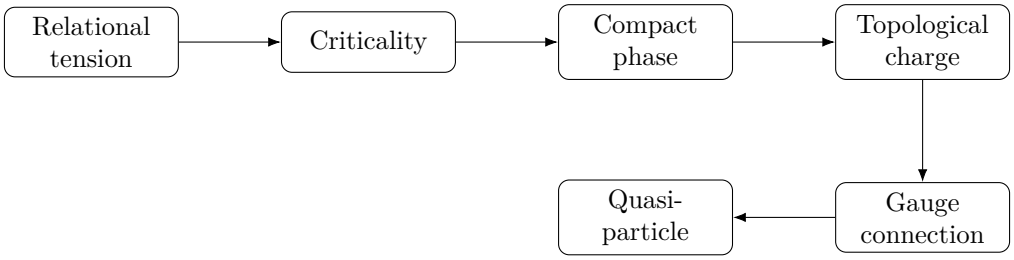

Figure 1: Conceptual route that survives the gates: pure tension produces pinned modes, while topology and a relational connection produce finite mass and conditional transport.

Table 2: Transport of a topological kink in a 1D relational network with disorder δ and weak adaptation η.

δ	η	displacement	final/initial width	energy drift	status
0.00	0	11.86	1.05	1.0×10^{-7}	passes
0.02	0	11.40	1.12	1.0×10^{-6}	passes
0.02	0.0003	9.73	1.13	1.3×10^{-2}	passes
0.05	0	10.16	1.41	1.0×10^{-6}	partial, 65%
0.05	0.0003	7.20	1.42	1.4×10^{-2}	partial, 50%
0.10	0	3.42	2.25	1.0×10^{-5}	fails

7 Energy–velocity relation: a consistency test, not RZS evidence

In the homogeneous sine-Gordon sector, the relation

$$E(v) = \gamma M_Q, \qquad \gamma = \frac{1}{\sqrt{1-v^2}}, \tag{13}$$

is expected from Lorentz invariance. Verifying it is not an RZS discovery. It only shows that the relativistic kink implementation is behaving correctly. RZS evidence begins when the same object is placed in disordered or adaptive W_i, and its stability becomes dependent on σ_{rel}.

8 Relational rigidity and the topological mass law

For $Q = 1$, the homogeneous test confirmed

$$M_1 = 8\sqrt{KU_0}. \tag{14}$$

Table 3: Topological mass law in the 1D sector.

K	U_0	measured M_Q	$8\sqrt{KU_0}$
0.25	0.25	1.99996	2.00000
0.50	1.00	5.65684	5.65685
1.00	1.00	7.99999	8.00000
2.00	1.00	11.31370	11.31371
4.00	4.00	31.99929	32.00000

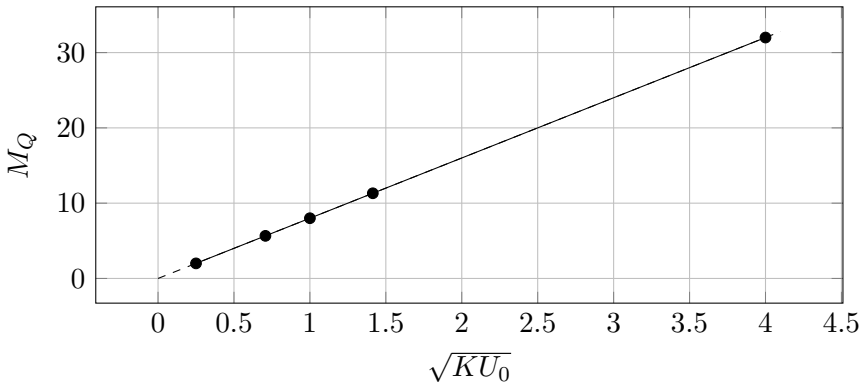

Figure 2: The topological mass scales linearly with $\sqrt{KU_0}$.

The connection with Romero stability was tested through an effective rigidity extracted from the mass:

$$K_{\text{eff}} = \frac{1}{U_0}\left(\frac{M_Q}{8}\right)^2. \tag{15}$$

With global operational definitions

$$B = \langle W_i \rangle, \qquad I = 1 + \frac{\text{std}(W_i)}{\langle W_i \rangle}, \qquad \tau = \frac{1}{\lambda_2(L_W)}, \tag{16}$$

I use

$$\widehat{\sigma}_{\text{rel}} = \frac{\lambda_2(L_W)}{I\lambda_{2,\text{hom}}}. \tag{17}$$

Here $\lambda_{2,\text{hom}}$ is the algebraic connectivity of the reference graph with the same topology, the same number of nodes, the same boundary conditions, and homogeneous weights equal to the mean $B = \langle W \rangle$:

$$\lambda_{2,\text{hom}} \equiv \lambda_2(L_{W_{ij}=B}). \tag{18}$$

In the 1D tests, this means the same chain or ring, with every link set to B; in the 2D tests, it means the same mesh and boundary conditions used in the corresponding experiment. With this normalization, $\widehat{\sigma}_{\text{rel}} = 1$ for the homogeneous reference medium when $I = 1$. The pilot fit, empirical and not derived from first principles, indicated $K_{\text{eff}} \sim \sqrt{\widehat{\sigma}_{\text{rel}}}$, with smaller error when stability was measured locally on the support of the soliton.

9 Internal modes and family structure

The simple sine-Gordon potential did not generate an internal family. The minimal correction was to add compact harmonics:

$$U(\phi) = \sum_{k=1}^{K} U_k(1 - \cos k\phi). \tag{19}$$

One natural family used in the tests was

$$U_k = \frac{r^{k-1}}{k^2}, \qquad K = 5, \qquad r = 1.3. \tag{20}$$

In this class, three bound internal modes appeared below the continuum.

Table 4: Three internal modes in the compact multi-harmonic potential.

mode	λ_n	$\omega_n = \sqrt{\lambda_n}$	interpretation
1	1.610	1.269	robust bound mode
2	4.734	2.176	bound mode
3	8.753	2.959	near the continuum
continuum	9.043	3.007	threshold

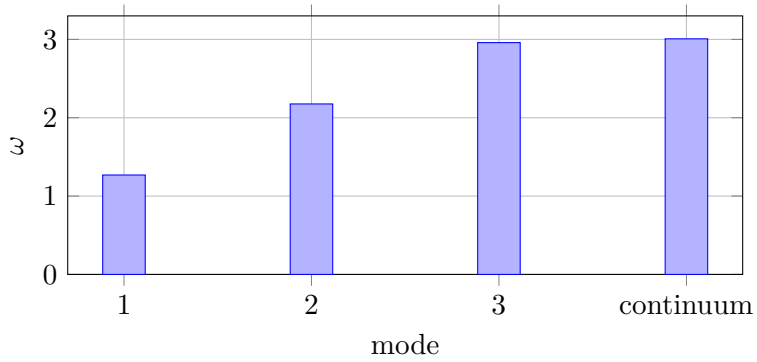

Figure 3: Bound internal modes below the continuum threshold.

The excitation energy of an internal mode obeyed, for small amplitudes,

$$\Delta E(A) \simeq \frac{1}{2}\omega_n^2 A^2. \tag{21}$$

This shows that internal modes are real degrees of freedom of the soliton. Classically, however, the amplitude A is continuous. Therefore, this does not automatically produce discrete family masses such as e, μ, τ.

10 Relation to lepton masses: negative result

The simplest attempt to produce an electron–muon–tau-like hierarchy failed. The observed ratios are very large:

$$\frac{m_\mu}{m_e} \approx 206.77, \qquad \frac{m_\tau}{m_e} \approx 3477.18. \tag{22}$$

A single harmonic internal mode, with consecutive levels,

$$M_n \approx M_0 + \hbar_{\text{eff}}\omega_{\text{int}}\left(n + \frac{1}{2}\right), \tag{23}$$

does not produce these ratios without choosing arbitrary levels. Thus, the identification with lepton families remains open and is not used as a conclusion.

11 Formal definition of wrap and 2D phase energy

A compact phase requires a well-defined angular difference modulo 2π. The operation used here is

$$\mathrm{wrap}(\Delta\theta) = \Delta\theta - 2\pi \left\lfloor \frac{\Delta\theta}{2\pi} + \frac{1}{2} \right\rfloor, \tag{24}$$

with image in the interval $[-\pi, \pi)$. Therefore, the relational XY energy is

$$E_{\mathrm{XY}} = \frac{K}{2} \sum_{\langle ij \rangle} W_{ij}\, \mathrm{wrap}(\theta_i - \theta_j)^2. \tag{25}$$

Intuition. The wrap operation prevents the phase from taking the wrong way around the circle. A phase difference of 2π is physically equivalent to zero. Without this rule, the energy of a vortex can be computed in a non-reproducible way.

12 2D without gauge fails: logarithmic energy

In the pure phase model, an isolated 2D vortex has growing energy:

$$E_{\mathrm{vortex}}(L) \sim \pi K \ln L. \tag{26}$$

This prevents it from being interpreted as an isolated particle of finite mass.

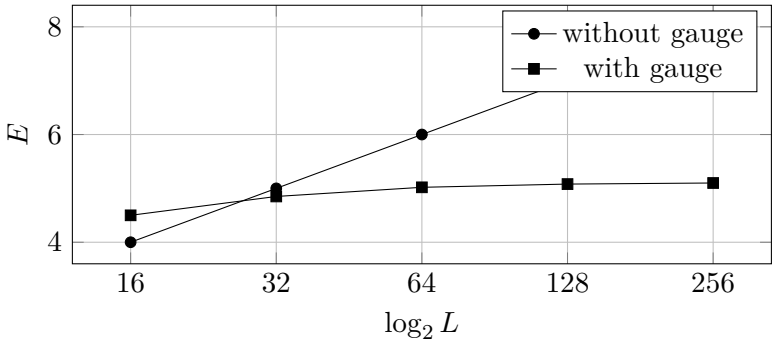

Figure 4: The global vortex grows with $\ln L$; the vortex with a gauge connection has finite energy.

13 2D with relational/gauge connection

The gauged energy used as the minimal 2D sector is

$$E = \sum_{\langle ij \rangle} KW_{ij} |\psi_i - e^{iA_{ij}} \psi_j|^2 + \frac{1}{2g^2} \sum_{\square} F_{\square}^2 + \sum_i \frac{\lambda}{4} (|\psi_i|^2 - 1)^2. \tag{27}$$

This convention uses the same $\lambda/4$ factor as the standard Abelian Higgs/Nielsen–Olesen form. If an implementation writes the potential as $(\lambda'/2)(|\psi|^2 - 1)^2$, then the parameters are related by $\lambda = 2\lambda'$. This observation is necessary when comparing values of λ with the literature. The connection A_{ij} cancels the phase twist away from the core. Geometrically, the covariant term wants

$$D\psi = (\nabla - iA)\psi \to 0 \tag{28}$$

outside the core. This makes the energy converge.

14 2D normalization audit

Some 2D energies belong to different functionals. Table 5 keeps the labels explicit.

Table 5: 2D normalizations. The values should not be compared directly.

Symbol	What it measures	typical value
E_{ansatz}	Energy of a gauged vortex with a static ansatz and the energy normalization used in the finite-mass test.	8.0809
E_{radial}	Relaxed radial energy in an adjusted continuous normalization; used to check radial stability.	≈ 6.28
E_{lattice}	Energy of the discrete Hamiltonian used in the gauge-Hamiltonian integrator. It includes its own factors of 1/2 and discretization.	3.4975

The number 8.0809 does not contradict 3.4975; they belong to different normalizations. For a final comparison, all tests should be repeated in a single discrete normalization.

15 Discrete Hamiltonian and Gauss constraint

The dynamical 2D sector uses variables ψ_i, links $U_{ij} = e^{iA_{ij}}$, electric fields E_{ij}, and momenta π_i:

$$H = \frac{1}{2}\sum_i |\pi_i|^2 + \frac{1}{2}\sum_{\langle ij\rangle} E_{ij}^2 + \frac{1}{2}\sum_{\langle ij\rangle} W_{ij}|\psi_i - e^{iA_{ij}}\psi_j|^2 + \frac{1}{2}\sum_{\square} F_{\square}^2 + \frac{1}{4}\sum_i (|\psi_i|^2 - 1)^2. \tag{29}$$

The Gauss constraint is

$$G_i = \operatorname{div} E_i - \operatorname{Im}(\pi_i^* \psi_i) = 0. \tag{30}$$

An integrator that does not conserve G_i cannot be used to claim vortex mobility. The projection used here corrects E by solving

$$\Delta\chi = G, \tag{31}$$

and applying

$$E'_{ij} = E_{ij} - \nabla\chi. \tag{32}$$

16 2D pinning and path stability

The gauged vortex has finite mass, but the relational medium creates pinning barriers. The barrier grows with disorder and is much larger when the disorder is correlated.

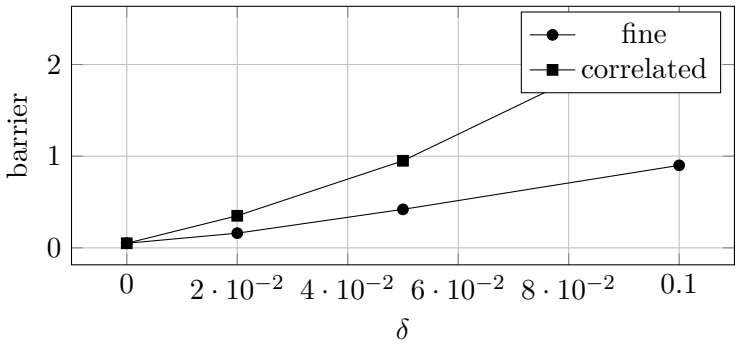

Figure 5: Pinning barriers for fine and correlated disorder.

This motivates distinguishing global stability from path stability:

$$\widehat{\sigma}_g > \sigma_c, \qquad \widehat{\sigma}_{\text{path}} > \sigma_c. \tag{33}$$

In the pilot test, a simple rule was

$$\widehat{\sigma}_g > 0.86, \qquad \widehat{\sigma}_{\text{path}} > 0.86. \tag{34}$$

It worked better than using global stability alone.

17 Current state of the 2D gates

The 2D route has both progress and bottlenecks. The static gauged vortex has finite mass. The stationary vortex, re-relaxed in the same discrete Hamiltonian, was stable. The Gauss projection works. The initial gauge-compatible boost has also been constructed. However, full dynamical 2D mobility has not yet been demonstrated.

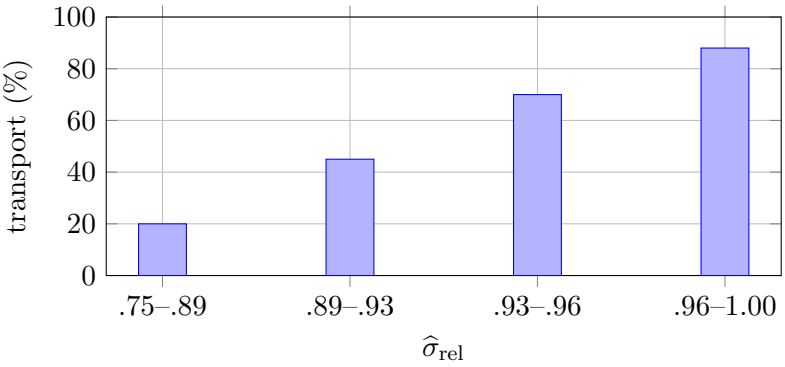

Figure 6: Transport rate by normalized Romero-stability band in a pilot test.

Table 6: Current 2D gates.

Gate	Status	Comment
Global 2D vortex	failed	energy grows as $\ln L$
Static gauged vortex	passed	finite energy
Static relational disorder	partially passed	finite mass, dispersion grows with δ
Collective-coordinate pinning	passed as a diagnostic	barriers depend on δ and correlation
Gauge-Hamiltonian integrator without vortex	passed	energy and Gauss constraint preserved
Stationary vortex in the discrete Hamiltonian	passed	core and topology preserved
Phase/boost perturbations	open	require gauge-compatible boost and energy control
Full 2D mobility	not demonstrated	next real gate

18 Conclusion

The central conclusion is restricted and, for that reason, stronger:

Relational tension alone did not generate mobile particles; it generated criticality, localization, and pinned defects. The route that survived requires compact phase, topological charge, and a relational/gauge connection. In the 1D sector, this produces solitons with mass, charge, mobility, interaction, internal modes, and Romero stability. In 2D, the gauge connection makes the mass finite, but full mobility remains an open numerical and physical problem.

The most important result is not an identification with real particles. It is the discovery of a candidate architecture:

$$(W, \theta, A, Q, \sigma_{\mathrm{rel}}) \longrightarrow \text{relational topological quasi-particle.} \tag{35}$$

To turn this architecture into a particle theory, at least five steps remain: full 2D dynamics, spin, couplings, quantization of internal modes, and connection with real particle data.

A Reproducible pseudocode for the main gates

1D transport gate

1. Define $W_i = 1 + \delta\xi_i$.
2. Initialize a kink with $Q = 1$.
3. Evolve with initial velocity v.
4. Measure Q, energy, center, width, and drift.
5. Repeat for weak η using $W_i \leftarrow W_i e^{-\eta T_i \Delta t}$.

Romero stability gate

1. Compute $B = \langle W \rangle$.
2. Compute $I = 1 + \mathrm{std}(W)/\langle W \rangle$.
3. Compute $\tau = 1/\lambda_2(L_W)$.
4. Build the homogeneous reference graph with the same topology and weights $W_{ij} = B$.
5. Compute $\lambda_{2,\mathrm{hom}} = \lambda_2(L_{W_{ij}=B})$.
6. Define $\widehat{\sigma} = \lambda_2(L_W)/(I\lambda_{2,\mathrm{hom}})$.
7. Compare transport with $\widehat{\sigma}_g$ and $\widehat{\sigma}_{\mathrm{path}}$.

2D gauge-Hamiltonian gate

1. Relax ψ, A in the same discrete Hamiltonian used for evolution.
2. Verify $|Q| = 1$ and finite energy.
3. Evolve without boost and require conservation of H and G_i.
4. Construct the boost by $\pi_{m,n} = -vD_x^{(c)}\psi_{m,n}$, using the central covariant difference

$$D_x^{(c)}\psi_{m,n} = \frac{U_{m,n;x}\psi_{m+1,n} - U^*_{m-1,n;x}\psi_{m-1,n}}{2a}, \tag{36}$$

   with lattice spacing $a = 1$ in the tests reported here and periodic indices whenever the boundary condition is periodic.
5. Solve $\mathrm{div}\, E = \mathrm{Im}(\pi^*\psi)$ to enforce $G_i = 0$.
6. Evolve and measure core, charge, energy, and displacement.

References

[1] F. G. Romero, *The Romero Law of Relational Stability (RZS): A Closed-Form Statement, Cross-Domain Operationalization, and Computational Verification*, PhilArchive/Zenodo, 2026. https://philarchive.org/rec/ROMTRL

[2] F. G. Romero, *The Canonical Closure of the RZS Framework*, PhilArchive/Zenodo, 2026. https://philarchive.org/rec/ROMTCC

[3] F. G. Romero, *From Weighted Microscopic Jumps to Operational Geometry in RZS*, PhilPapers/PhilArchive, 2026. https://philpapers.org/archive/ROMFWM.pdf

[4] R. K. Dodd, J. C. Eilbeck, J. D. Gibbon, and H. C. Morris, *Solitons and Nonlinear Wave Equations*, Academic Press, 1982.

[5] H. B. Nielsen and P. Olesen, "Vortex-line models for dual strings," *Nuclear Physics B* **61**, 45–61, 1973. https://doi.org/10.1016/0550-3213(73)90350-7

[6] J. M. Kosterlitz and D. J. Thouless, "Ordering, metastability and phase transitions in two-dimensional systems," *Journal of Physics C* **6**, 1181, 1973.

[7] Y. Koide, "New view of quark and lepton mass hierarchy," *Physical Review D* **28**, 252, 1983. https://doi.org/10.1103/PhysRevD.28.252

[8] Particle Data Group, *Review of Particle Physics / Particle Listings*, 2025. https://pdg.lbl.gov/2025/listings/particle_properties.html